

# UC Irvine

## UC Irvine Previously Published Works

### Title

Combining a Nitrogenase Scaffold and a Synthetic Compound into an Artificial Enzyme

### Permalink

<https://escholarship.org/uc/item/53c8x1k5>

### Journal

Angewandte Chemie International Edition, 54(47)

### ISSN

1433-7851

### Authors

Tanifuji, Kazuki  
Lee, Chi Chung  
Ohki, Yasuhiro  
[et al.](#)

### Publication Date

2015-11-16

### DOI

10.1002/anie.201507646

Peer reviewed



# HHS Public Access

Author manuscript

*Angew Chem Int Ed Engl.* Author manuscript; available in PMC 2016 November 16.

Published in final edited form as:

*Angew Chem Int Ed Engl.* 2015 November 16; 54(47): 14022–14025. doi:10.1002/anie.201507646.

## Combining a Nitrogenase Scaffold and a Synthetic Compound into an Artificial Enzyme\*\*

**Dr. Kazuki Tanifuji,**

Department of Molecular Biology and Biochemistry, University of California, Irvine, Irvine, CA 92697-3900

**Dr. Chi Chung Lee,**

Department of Molecular Biology and Biochemistry, University of California, Irvine, Irvine, CA 92697-3900

**Prof. Dr. Yasuhiro Ohki,**

Department of Chemistry, Graduate School of Science and Research Center for Materials Science, Nagoya University, Furo-cho, Chikusa-ku, Nagoya 464-8602 (Japan)

**Prof. Dr. Kazuyuki Tatsumi,**

Department of Chemistry, Graduate School of Science and Research Center for Materials Science, Nagoya University, Furo-cho, Chikusa-ku, Nagoya 464-8602 (Japan)

**Prof. Dr. Yilin Hu\***, and

Department of Molecular Biology and Biochemistry, University of California, Irvine, Irvine, CA 92697-3900

**Prof. Dr. Markus W. Ribbe\***

Department of Molecular Biology and Biochemistry; Department of Chemistry, University of California, Irvine, Irvine, CA 92697-3900

### Abstract

Nitrogenase catalyzes substrate reduction at its cofactor center ( $[(\text{Cit})\text{MoFe}_7\text{S}_9\text{C}]^{\text{n-}}$ ; designated M-cluster). Here, we report the formation of an artificial, nitrogenase-mimicking enzyme upon insertion of a synthetic model complex ( $[\text{Fe}_6\text{S}_9(\text{SEt})_2]^{4-}$ ; designated  $\text{Fe}_6^{\text{RHH}}$ ) into the catalytic component of nitrogenase (designated NifDK). Two  $\text{Fe}_6^{\text{RHH}}$  clusters were inserted into NifDK, rendering the resultant protein (designated NifDK<sup>Fe</sup>) in a similar conformation to that upon insertion of native M-clusters. NifDK<sup>Fe</sup> could work together with the reductase component of nitrogenase to reduce  $\text{C}_2\text{H}_2$  in an ATP-dependent reaction. It could also act as an enzyme on its own in the presence of Eu(II) DTPA, displaying a strong activity in  $\text{C}_2\text{H}_2$  reduction while demonstrating an ability to reduce  $\text{CN}^-$  to C1-C3 hydrocarbons in an ATP-independent manner.

\*\*This work was supported by NIH grant GM-67626 (M.W.R.) and Grant-in-Aids for Scientific Research from the Ministry of Education, Culture, Sports, Science and Technology, Japan, No. 25109522 (Y.O.) and No. 23000007 (K.T.).

\*yilinh@uci.edu, mribbe@uci.edu.

Supporting information for this article, including experimental procedures, Table S1 and Figures S1-S3, is given via a link at the end of the document.

The successful outcome of this work provides the proof of concept and underlying principles for continued search of novel enzymatic activities via this approach.

## Keywords

nitrogenase; artificial enzyme; synthetic compound; C-C coupling; hydrocarbon

Nitrogenase is a structurally complex and functionally versatile metalloenzyme that catalyzes the reduction of a variety of substrates, including dinitrogen ( $N_2$ ), acetylene ( $C_2H_2$ ), cyanide ions ( $CN^-$ ), carbon monoxide (CO) and carbon dioxide ( $CO_2$ ), under ambient conditions.<sup>[1-7]</sup> Among these reactions, the reduction of  $N_2$  to ammonia ( $NH_3$ ) represents a key step in the global nitrogen cycle; whereas the conversion of  $CN^-$ , CO and  $CO_2$  to hydrocarbons provides an important template for future development of strategies to recycle carbon wastes into useful carbon fuels.<sup>[8,9]</sup> The “conventional” molybdenum (Mo)-nitrogenase consists of two component proteins: a  $\gamma_2$ -dimeric reductase (designated NifH), which houses a subunit-bridging  $[Fe_4S_4]$  cluster and an ATP-binding site within each subunit; and a  $\alpha_2\beta_2$ -tetrameric catalytic component (designated NifDK), which contains a P-cluster ( $[Fe_8S_7]$ ) at the  $\alpha/\beta$ -subunit interface and an M-cluster ( $[(Cit)MoFe_7S_9C]$ ; Cit, homocitrate) within each  $\alpha$ -subunit (Figure S1A). Catalysis by Monitrogenase is enabled by the formation of a functional complex between NifH and NifDK,<sup>[10]</sup> and the subsequent ATP-dependent transfer of electrons from the  $[Fe_4S_4]$  cluster of NifH, via the P-cluster, to the M-cluster of NifDK, where substrate reduction occurs (Figure S1A).

The M-cluster ( $[(Cit)MoFe_7S_9C]^{n-}$ ) can be viewed as  $[MoFe_3S_3]$  and  $[Fe_4S_3]$  subclusters bridged by three  $\mu_2$ -“belt” sulfur (S) atoms and a  $\mu_6$ -interstitial carbide ( $C^{4-}$ ) atom; in addition, it is coordinated by an organic compound, homocitrate, at its Mo end (Figure 1A).<sup>[11-13]</sup> This unique metallocluster has attracted the attention of synthetic chemists and chemical biologists alike and prompted a joint search between them for a synthetic mimic of the M-cluster that could be combined with an appropriate protein scaffold into a functional enzyme. One synthetic compound has come into sight as a potential candidate for this line of investigation. First reported by the Holm group in 1981, this  $[Fe_6S_9(SET)_2]^{4-}$  cluster (designated  $Fe_6^{RHH}$ , Et, ethyl) is a hexanuclear Fe-S-thiolate cluster with non-cuboidal geometry and rhomb faces.<sup>[14,15]</sup> Compared to the M-cluster (Figure 1A; *also see* Figure S2),  $Fe_6^{RHH}$  has a Fe atom substituting for the Mo atom and the homocitrate moiety at one end of the cluster; moreover, it “misses” two  $\mu_4$ -Fe atoms and has a  $\mu_4$ -bridging S atoms instead of the  $\mu_6$ -interstitial C atom in the “center” of the cluster (Figure 1B; *also see* Figure S2). Strikingly, despite these differences,  $Fe_6^{RHH}$  bears a remarkable resemblance to the M-cluster in the overall geometry, overlaying well with the structure of the M-cluster except for the absence of one of the three “Fe faces” of the cofactor (Figure 1C). Additionally, the anionic nature of  $Fe_6^{RHH}$  mimics that of the M-cluster, which is believed to be crucial for incorporation of the cofactor along a positively charged insertion path into NifDK (Figure 1D).<sup>[16]</sup> Finally,  $Fe_6^{RHH}$  is known to undergo facile ligand substitutions,<sup>[14,15]</sup> which could facilitate exchange of the ethanethiol ligand of  $Fe_6^{RHH}$  with the M-cluster ligands, Cys<sup>a275</sup> and His<sup>a442</sup>, at the cofactor-binding site of NifDK.

Indeed,  $\text{Fe}_6^{\text{RHH}}$  could be inserted into the cofactor-deficient form of NifDK (designated NifDK<sup>apo</sup>), resulting in an artificial catalytic component of nitrogenase with a synthetic cofactor center. Metal analysis revealed an increase of the Fe content from  $15.2 \pm 1.4$  to  $27.2 \pm 0.1$  mol Fe/mol protein before and after NifDK<sup>apo</sup> was incubated with  $\text{Fe}_6^{\text{RHH}}$  (Table S1), suggesting the formation of a  $\text{Fe}_6^{\text{RHH}}$ -reconstituted form of NifDK (designated NifDK<sup>Fe</sup>) upon such a treatment. Subtraction of the Fe content of NifDK<sup>apo</sup> (each containing two P-clusters) from that of NifDK<sup>Fe</sup> (each containing two P-clusters plus two  $\text{Fe}_6^{\text{RHH}}$ ) indicated “acquisition” of approximately 12 mol Fe/mol protein by NifDK<sup>Fe</sup>, which would be consistent with the incorporation of two  $\text{Fe}_6^{\text{RHH}}$  (each containing six Fe atoms) into the two cofactor-binding sites in NifDK (*see* Figure S1A). Treatment of NifDK<sup>Fe</sup> and NifDK<sup>M</sup> (*i.e.*, an M-cluster-reconstituted form of NifDK) by an iron chelator, bathophenan-throline disulfonate, resulted in chelation of  $12.3 \pm 0.7$  and  $12.2 \pm 1.1$  mol Fe/mol protein, respectively. These chelation-accessible Fe atoms likely originated from the unprotected Fe atoms of the P-cluster, particularly given the relatively exposed location of this cluster at the  $\alpha/\beta$ -subunit interface of NifDK (*see* Figure S1A). More importantly, the nearly identical amounts of accessible Fe atoms in NifDK<sup>Fe</sup> and NifDK<sup>M</sup> implied that the two proteins had similar flexibility in the protein environments surrounding the clusters that rendered similar accessibility of the cluster Fe atoms to the Fe chelator. One account for such a similarity could be a similar conformation assumed by the two proteins upon incorporation of their respective cofactors. In this scenario, NifDK<sup>Fe</sup> and NifDK<sup>M</sup> could form similar complexes with NifH, which would enable analogous ATP-dependent electron transfer within the complexes for the subsequent substrate reduction at their respective cofactor sites (*see* Figure S1A).

Consistent with this suggestion, NifDK<sup>Fe</sup> was capable of reducing acetylene ( $\text{C}_2\text{H}_2$ ) to ethylene ( $\text{C}_2\text{H}_4$ ) when it was combined with NifH, ATP and dithionite (Figure 2A, ①), forming 164 nmol  $\text{C}_2\text{H}_4$ /mg protein (equivalent to 36 turnovers) over a time period of 30 minutes (Figure 2A, *inset*). This activity originated from  $\text{Fe}_6^{\text{RHH}}$ , as no activity was observed prior to insertion of  $\text{Fe}_6^{\text{RHH}}$  into NifDK<sup>apo</sup> (Figure 2A, ②). Further, NifDK<sup>Fe</sup> was inactive in the reaction of  $\text{C}_2\text{H}_2$  reduction when ATP (Figure 2A, ③) or NifH (Figure 2A, ④) was omitted. The specific activity of ATP-dependent  $\text{C}_2\text{H}_2$  reduction by NifDK<sup>Fe</sup> ( $23.7 \pm 0.4$  nmol  $\text{C}_2\text{H}_4$ /mg protein/min) was only 2% of that by NifDK<sup>M</sup> ( $1057 \pm 55$  nmol  $\text{C}_2\text{H}_4$ /mg protein/min), reflecting a structural/redox difference between  $\text{Fe}_6^{\text{RHH}}$  and the M-cluster (*see* Figure 1) and/or an “imperfect” alignment of  $\text{Fe}_6^{\text{RHH}}$  with other components along the electron transfer pathway upon docking of NifH on NifDK<sup>Fe</sup> (*see* Figure S1A). Nevertheless, the observed ATP- and reductase-dependence, as well as the ability to reduce  $\text{C}_2\text{H}_2$ , established NifH/NifDK<sup>Fe</sup> as an analogous two-component enzymatic system to the native nitrogenase (*i.e.*, NifH/NifDK<sup>M</sup>). Interestingly, when combined with Eu(II) DTPA ( $E^{\circ} = -1.14$  V at pH 8) in an aqueous buffer, NifDK<sup>Fe</sup> was able to catalyze the reduction of  $\text{C}_2\text{H}_2$  to  $\text{C}_2\text{H}_4$  at a much higher efficiency in the absence of ATP and NifH (Figure 2B, ①), forming 4758 nmol  $\text{C}_2\text{H}_4$ /mg protein within the first 2 minutes and reaching a maximum product formation of 5460 nmol  $\text{C}_2\text{H}_4$ /mg protein (equivalent to 1213 turnovers) over a time period of 10 minutes (Figure 2B, *inset*). Neither  $\text{Fe}_6^{\text{RHH}}$  (Figure 2B, ③) nor NifDK<sup>apo</sup> (Figure 2B, ④) alone showed activity of  $\text{C}_2\text{H}_2$  reduction in the Eu(II) DTPA-driven reaction, suggesting that the activity was achieved only upon incorporation of  $\text{Fe}_6^{\text{RHH}}$  into

NifDK. Moreover, NifDK<sup>Fe</sup> was twice as active as NifDK<sup>M</sup> in ATP-independent C<sub>2</sub>H<sub>2</sub> reduction (Figure 2B, ②), showing an activity normally achieved by the wild-type NifDK in ATP-dependent C<sub>2</sub>H<sub>2</sub> reduction.<sup>[17]</sup> Together, these observations demonstrated the ability of NifDK<sup>Fe</sup> to function as an efficient, artificial C<sub>2</sub>H<sub>2</sub> reductase on its own (*see* Figure S1B).

The observation of strong reactivity of NifDK<sup>Fe</sup> toward C<sub>2</sub>H<sub>2</sub> compelled us to further explore the reactivity of this artificial enzyme toward other carbon-containing compounds, such as cyanide ions (CN<sup>-</sup>), in ATP-independent reactions. Driven by Eu(II) DTPA, NifDK<sup>Fe</sup> was capable of reducing CN<sup>-</sup> to C1-C3 hydrocarbons at a total of 168 nmol reduced C/mg protein (equivalent to 37 turnovers) over a time period of 90 minutes (Figure 3A, ●); in contrast, no hydrocarbon product was generated by NifDK<sup>apo</sup> in the same, Eu(II) DTPA-driven reaction (Figure 3A, ○), suggesting that the activity of CN<sup>-</sup> reduction was associated with the NifDK-bound **Fe<sub>6</sub><sup>RHH</sup>**. Gas chromatograph-mass spectrometry (GC-MS) analysis further confirmed CN<sup>-</sup> as the source of carbon in the hydrocarbon products, showing expected mass shifts of +1, +2 and +3, respectively, of C1 (CH<sub>4</sub>), C2 (C<sub>2</sub>H<sub>4</sub>, C<sub>2</sub>H<sub>6</sub>) and C3 (C<sub>3</sub>H<sub>6</sub>, C<sub>3</sub>H<sub>8</sub>) products upon substitution of <sup>13</sup>CN<sup>-</sup> for <sup>12</sup>CN<sup>-</sup> (Figure 3B, *upper vs. lower*). It is interesting to note that reduction of CN<sup>-</sup> to hydrocarbons by NifDK<sup>Fe</sup> was accompanied by simultaneous formation of NH<sub>4</sub><sup>+</sup>; however, the amount of N in NH<sub>4</sub><sup>+</sup> (8.1 ± 1.1 nmol N/mg protein/min) was 1.8-fold in excess (as opposed to being equivalent) to the total amount of C in hydrocarbon products that were detected in this reaction (4.4 ± 0.6 nmol reduced C/mg protein/min). IC-MS analysis indicated that all detected NH<sub>4</sub><sup>+</sup> was generated from the reduction of CN<sup>-</sup> (Figure S3), suggesting the formation of other carbon-containing products (up to 44%) that remained to be identified to complete the total C count of CN<sup>-</sup>-reduction.

The results of this study provide the first proof-of-concept for combining a nitrogenase protein scaffold with a complex, synthetic metal-sulfur cofactor into an artificial enzyme. While this case deals specifically with a “nitrogenase mimic”, several “compatibility parameters”, such as the electrostatic interaction that facilitates insertion of **Fe<sub>6</sub><sup>RHH</sup>** along the cofactor-insertion path, the suitable geometry that permits occupancy of **Fe<sub>6</sub><sup>RHH</sup>** at the cofactor-binding site, and the facile ligands that enable coordination of **Fe<sub>6</sub><sup>RHH</sup>** by protein ligands upon ligand-exchange, represent some general principles that are most important for the success of this line of work. With regard to the NifDK<sup>apo</sup> scaffold, it not only protects and stabilizes **Fe<sub>6</sub><sup>RHH</sup>** in aqueous solutions, but also gives the protein-bound **Fe<sub>6</sub><sup>RHH</sup>** a certain substrate selectivity that is characteristic of enzymatic systems. As far as **Fe<sub>6</sub><sup>RHH</sup>** is concerned, it was shown to undergo a reversible one-electron transfer at -0.38 V *vs.* SHE and an irreversible one-electron transfer at -1.42 V *vs.* SHE in dimethyl sulfoxide (DMSO);<sup>[14,15]</sup> and the oxidation states of its Fe atoms were described as 4Fe(III) and 2Fe(II), with electrons delocalized among these atoms.<sup>[14,18]</sup> Interestingly, these parameters are loosely analogous to those of the solvent-extracted M-cluster,<sup>[19-21]</sup> further highlighting an inherent structural-functional analogy between the two clusters.

Despite the absence of one “Fe face”, **Fe<sub>6</sub><sup>RHH</sup>** still “retains” two μ<sub>2</sub>-S atoms that have a similar spatial arrangement to that of the μ<sub>2</sub>-“belt” S atoms of the M-cluster; moreover, it has a μ<sub>4</sub>-S atom that occupies a similar location to that of the μ<sub>6</sub>-“central” C atom in the M-cluster (*see* Figure 1C). Preservation of these features may be crucial for the reactivity of

$\text{Fe}_6^{\text{RHH}}$ , as a recent crystallographic study revealed displacement of a “belt” S atom by a CO moiety upon binding of CO to the M-cluster,<sup>[22]</sup> an event requiring the presence of the interstitial C atom to maintain the structural integrity of the M-cluster when the S “belt” undergoes significant rearrangement during catalysis. Thus, by analogy, the equivalents to the “belt” S and “central” C atoms in  $\text{Fe}_6^{\text{RHH}}$  may render it capable of interacting with substrates in an analogous manner to that of the M-cluster; in particular, such an analogy could explain the reactivity of  $\text{Fe}_6^{\text{RHH}}$  toward  $\text{CN}^-$ , which parallels the reactivity of the M-cluster toward CO (an isoelectronic molecule to the  $\text{CN}^-$  ion), in reductive C-C coupling.<sup>[2-4]</sup> On the other hand, the unique structural features of  $\text{Fe}_6^{\text{RHH}}$  results in the distinct catalytic profile of  $\text{NifDK}^{\text{Fe}}$ , such as improved activities of  $\text{C}_2\text{H}_2^-$  and  $\text{CN}^-$ -reduction when it acts on its own as an enzyme. It is conceivable, therefore, that a continued effort to incorporate other synthetic cofactor variants into a suitable protein scaffold will not only advance mechanistic understanding of nitrogenase from a different viewpoint, but also facilitate identification of novel enzymatic activities that may be useful in a practical vein.

The  $\text{Fe}_6^{\text{RHH}}$  cluster came from a long line of synthetic compounds that were generated in a quest for synthetic routes to nitrogenase-based, biomimetic metal clusters.<sup>[23-26]</sup> Such a quest began even before the structures of the nitrogenase clusters were known, when a variety of relatively small FeS clusters, including cubane-type FeS clusters with various ligands (and, in some cases, heterometals), were synthesized and characterized.<sup>[15,23]</sup> As chemical and spectroscopic information of the nitrogenase clusters became available, much effort has been focused on generation of high-nuclearity metaloclusters. The previously-synthesized MoFeS and VFeS clusters with phosphine ligands were utilized as instrumental building blocks in a fusion strategy that led to edge-bridged double-cubane clusters<sup>[23,24]</sup> and, subsequently, core conversion and ligand exchange/removal strategies were developed that resulted in  $\text{P}^{\text{N}}$ - and M-type topologs.<sup>[25]</sup> The successful synthesis of these clusters not only provides the much-needed model compounds that mimic the nitrogenase clusters in structural and redox properties, but also reveals a certain parallelism between the classic synthetic strategy<sup>[24,25]</sup> and the biosynthetic mechanisms utilized by nitrogenase clusters<sup>[27]</sup> in fusing small FeS units into larger FeS cores. A similar concept was successfully applied to the generation of a functional, semisynthetic hydrogenase.<sup>[28,29]</sup> Interestingly, a different synthetic approach emerged in recent years, which led to synthesis of a series of FeS clusters, including two 8Fe mimics of nitrogenase clusters, via spontaneous condensation of iron and sulfido monomeric units.<sup>[26]</sup> The observation of two different synthetic strategies leads to the speculation of whether the “prototype” of nitrogenase clusters originated from spontaneous reactions in the primordial, abiotic environment, which then evolved into a well-organized, protein scaffold-assisted mechanism that step-by-step fused small FeS units into high-nuclearity FeS clusters. Regardless of what evolutionary implications they may have, the chemical synthetic approaches will continue to evolve and add new members to the library of synthetic cofactors, assisting in our pursuit of artificial enzymes while providing relevant insights into the assembly and catalysis of nitrogenase.

## Supplementary Material

Refer to Web version on PubMed Central for supplementary material.

## References

1. Burgess BK, Lowe DJ. *Chem. Rev.* 1996; 96:2983–3012. [PubMed: 11848849]
2. Lee CC, Hu Y, Ribbe MW. *Science.* 2010; 329:642. [PubMed: 20689010]
3. Hu Y, Lee CC, Ribbe MW. *Science.* 2011; 333:753–755. [PubMed: 21817053]
4. Lee CC, Hu Y, Ribbe MW. *Angew. Chem. Int. Ed. Engl.* 2015; 54:1219–1222. [PubMed: 25420957]
5. Rebelein JG, Hu Y, Ribbe MW. *Angew. Chem. Int. Ed. Engl.* 2014; 53:11543–11546. [PubMed: 25205285]
6. Hoffman BM, Lukoyanov D, Yang ZY, Dean DR, Seefeldt LC. *Chem. Rev.* 2014; 114:4041–4062. [PubMed: 24467365]
7. Lee SC, Lo W, Holm RH. *Chem. Rev.* 2014; 114:3579–3600. [PubMed: 24410527]
8. Rofer-DePoorter CK. *Chem. Rev.* 1981; 81:447–474.
9. Gerlach DL, Lehnert N. *Angew. Chem. Int. Ed. Engl.* 2011; 50:7984–7986. [PubMed: 21761528]
10. Rees DC, Tezcan FA, Haynes CA, Walton MY, Andrade S, Einsle O, Howard JB. *Philos. Trans. A Math. Phys. Eng. Sci.* 2005; 363:971–984. [PubMed: 15901546]
11. Lancaster KM, Roemelt M, Ettenhuber P, Hu Y, Ribbe MW, Neese F, Bergmann U, DeBeer S. *Science.* 2011; 334:974–977. [PubMed: 22096198]
12. Spatzal T, Aksoyoglu M, Zhang L, Andrade SL, Schleicher E, Weber S, Rees DC, Einsle O. *Science.* 2011; 334:940. [PubMed: 22096190]
13. Wiig JA, Hu Y, Lee CC, Ribbe MW. *Science.* 2012; 337:1672–1675. [PubMed: 23019652]
14. Christou G, Holm RH, Sabat M, Ibers JA. *J. Am. Chem. Soc.* 1981; 103:6269–6271.
15. Hagen KS, Watson AD, Holm RH. *J. Am. Chem. Soc.* 1983; 105:3905–3913.
16. Schmid B, Ribbe MW, Einsle O, Yoshida M, Thomas LM, Dean DR, Rees DC, Burgess BK. *Science.* 2002; 296:352–356. [PubMed: 11951047]
17. Eady RR. *Chem. Rev.* 1996; 96:3013–3030. [PubMed: 11848850]
18. Strasdeit H, Krebs B, Henkel G. *Inorg. Chem.* 1984; 23:1816–1825.
19. Schultz FA, Gheller SF, Burgess BK, Lough S, Newton WE. *J. Am. Chem. Soc.* 1985; 107:5364–5368.
20. Burgess BK. *Chem. Rev.* 1990; 90:1337–1406.
21. Harris TV, Szilagyik RK. *Inorg. Chem.* 2011; 50:4811–4824. [PubMed: 21545160]
22. Spatzal T, Perez KA, Einsle O, Howard JB, Rees DC. *Science.* 2014; 345:1620–1623. [PubMed: 25258081]
23. Lee SC, Holm RH. *Proc. Natl. Acad. Sci. U. S. A.* 2003; 100:3595–3600. [PubMed: 12642670]
24. Lee SC, Holm RH. *Chem. Rev.* 2004; 104:1135–1158. [PubMed: 14871151]
25. Lee SC, Lo W, Holm RH. *Chem. Rev.* 2014; 114:3579–3600. [PubMed: 24410527]
26. Ohki Y, Tatsumi K. *Z. Anorg. Allg. Chem.* 2013; 639:1340–1349.
27. Ribbe MW, Hu Y, Hodgson KO, Hedman B. *Chem. Rev.* 2014; 114:4063–4080. [PubMed: 24328215]
28. Esselborn J, Lambert C, Adamska-Venkatesh A, Simmons T, Berggren G, Noth J, Siebel J, Hemschemeier A, Artero V, Reijerse E, Fontecave M, Lubitz W, Happe T. *Nat. Chem. Biol.* 2013; 9:607–609. [PubMed: 23934246]
29. Berggren G, Adamska A, Lambert C, Simmons TR, Esselborn J, Atta M, Gambarelli S, Muesca JM, Reijerse E, Lubitz W, Happe T, Artero V, Fontecave M. *Nature.* 2013; 499:66–69. [PubMed: 23803769]



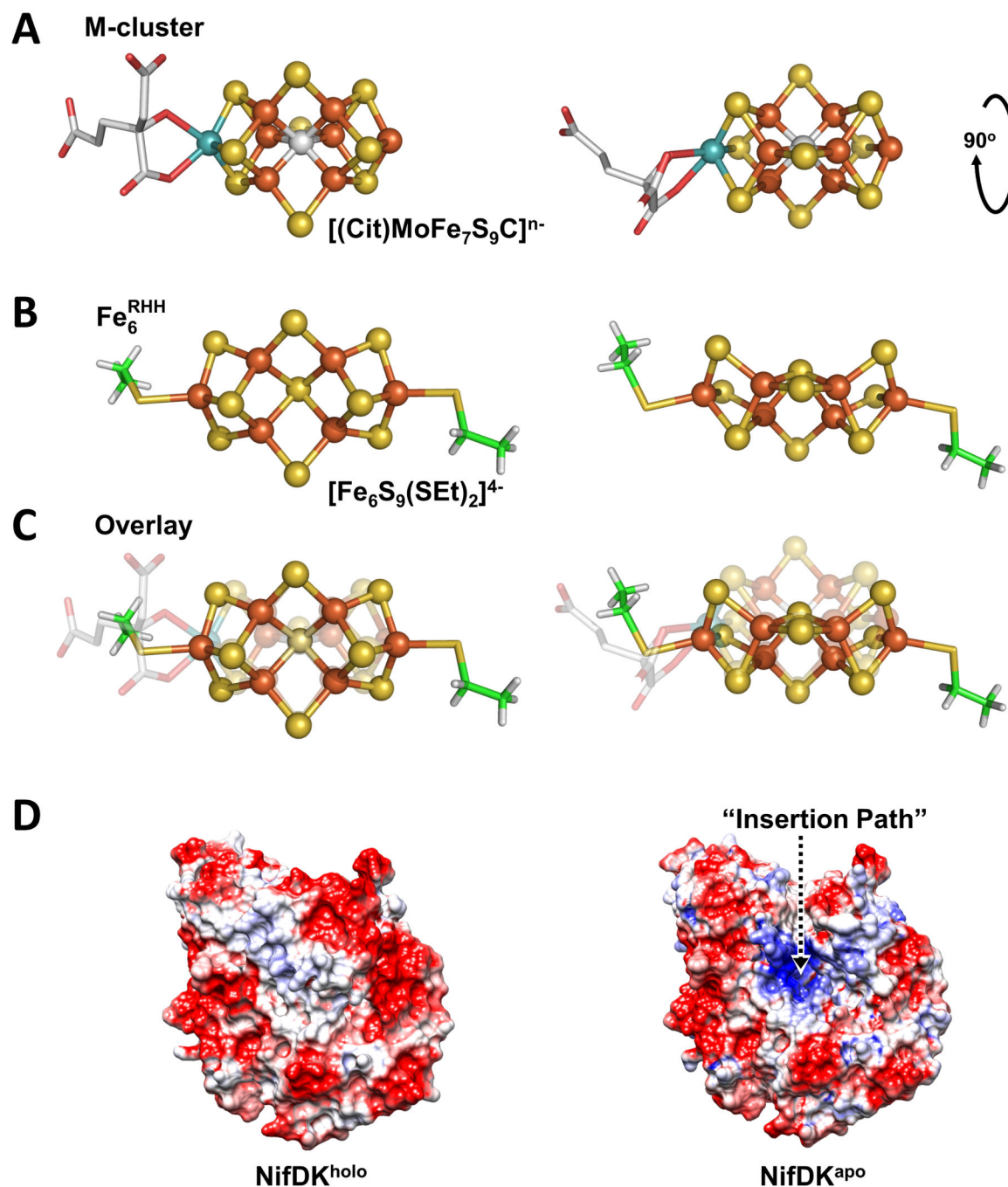


**Figure 1.** Nitrogenase cofactor, synthetic compound and protein scaffold. Structural models of the M-cluster (A) and the  $\text{Fe}_6^{\text{RHH}}$  compound (B), and the overlay of the two structures (C) in top (left) and side (right) views. PDB entry 3U7Q<sup>[12]</sup> and data from ref. 15 were used to generate these models. Atoms are colored as follows: Fe, orange; S, yellow; Mo, cyan; O, red; C (M-cluster), light gray; C ( $\text{Fe}_6^{\text{RHH}}$ ), green; H ( $\text{Fe}_6^{\text{RHH}}$ ), gray. (D) Comparison of the  $\alpha$ -subunits of the wild-type NifDK (NifDK<sup>holo</sup>) and the cofactor-deficient NifDK



(NifDK<sup>apo</sup>), which reveals the presence of a positively-charged cofactor-insertion path in NifDK<sup>apo</sup> (*right*) that is closed up in NifDK<sup>holo</sup> upon insertion of the cofactor (*left*).

Author Manuscript

Author Manuscript

Author Manuscript

Author Manuscript

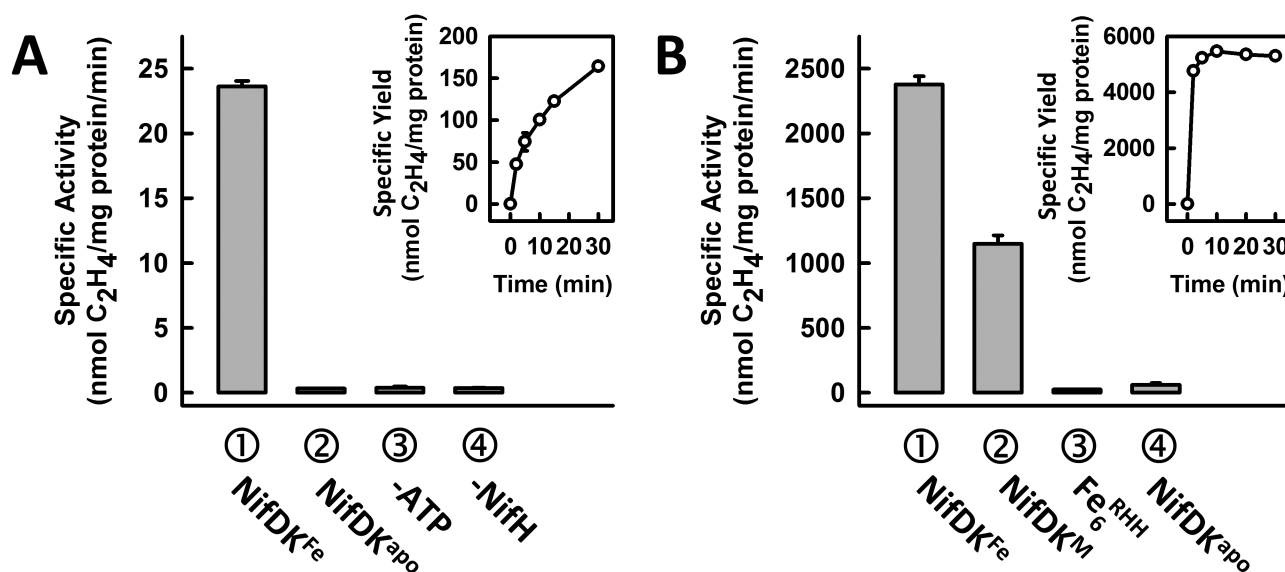


**Figure 2.**

C<sub>2</sub>H<sub>2</sub> reduction by NifDK<sup>Fe</sup> in ATP-dependent and independent reactions. (A) Specific activity of C<sub>2</sub>H<sub>4</sub> formation by NifDK<sup>Fe</sup> (①) or NifDK<sup>apo</sup> (②) from C<sub>2</sub>H<sub>2</sub> reduction in an assay containing NifH, ATP and dithionite; or by NifDK<sup>Fe</sup> in the same assay minus ATP (③) or NifH (④). Inset shows the time course of ATP-dependent C<sub>2</sub>H<sub>4</sub> formation by NifDK<sup>Fe</sup>. (B) Specific activity of C<sub>2</sub>H<sub>4</sub> formation by NifDK<sup>Fe</sup> (①), NifDK<sup>M</sup> (②), Fe<sub>6</sub><sup>RHH</sup> (③) or NifDK<sup>apo</sup> (④) from C<sub>2</sub>H<sub>2</sub> reduction in an assay containing Eu(II) DTPA. Inset shows the time course of ATP-independent C<sub>2</sub>H<sub>4</sub> formation by NifDK<sup>Fe</sup>. Data are shown as mean ± SD (*N* = 3).

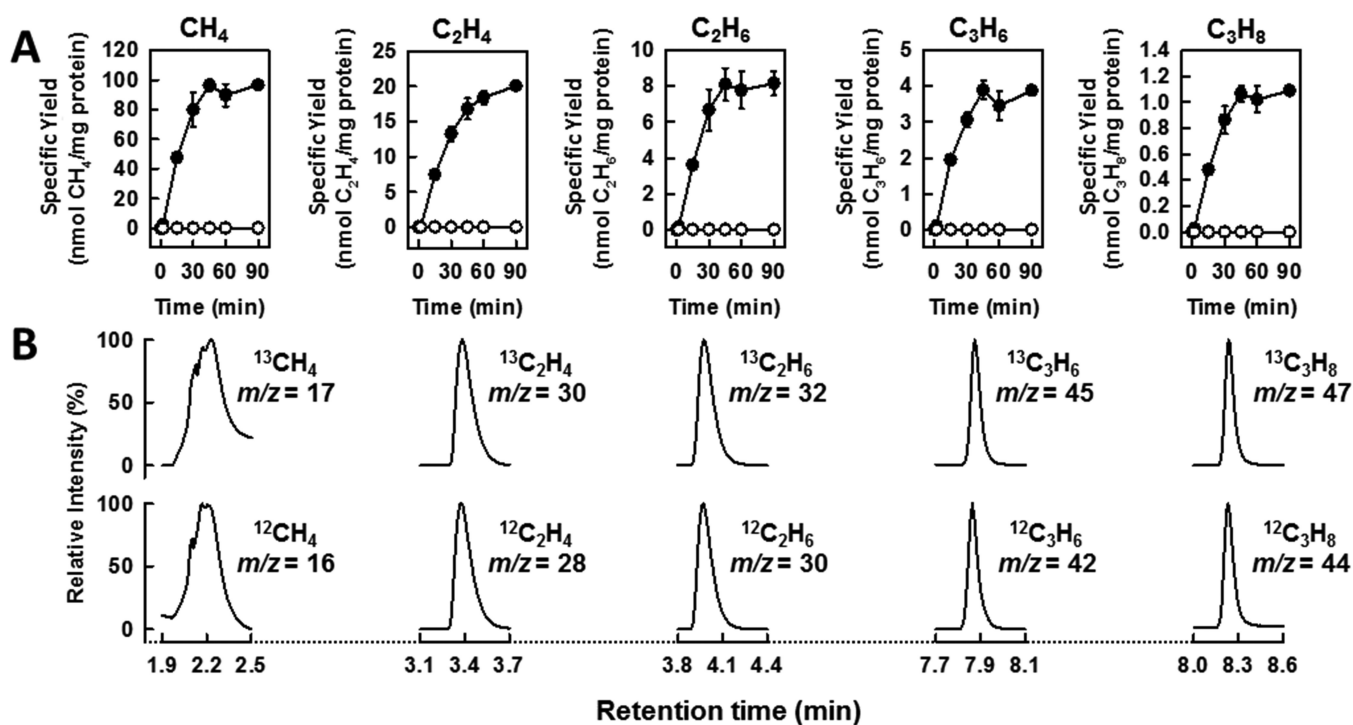


**Figure 3.**

ATP-independent  $\text{CN}^-$  reduction by  $\text{NifDK}^{\text{Fe}}$ . (A) Time courses of hydrocarbon formation by  $\text{NifDK}^{\text{Fe}}$  from  $\text{CN}^-$  reduction in an assay containing Eu(II) DTPA. (B) GC-MS analysis of hydrocarbon products formed by  $\text{NifDK}^{\text{Fe}}$  in the presence of Eu(II) DTPA when  $^{13}\text{CN}^-$  (upper) or  $^{12}\text{CN}^-$  (lower) was supplied as a substrate.